Broadband antihole photon sieve telescope

Geoff Andersen* and Drew Tullson

Laser and Optics Research Center, HQ USAFA/DFP, Suite 2A31, 2354 Fairchild Drive, U.S. Air Force Academy, Colorado 80840, USA

*Corresponding author: geoff.andersen@usafa.af.mil

Received 18 December 2006; accepted 6 February 2007;
posted 21 February 2007 (Doc. ID 78186); published 31 May 2007

A broadband-corrected optical telescope has been constructed from a photon sieve with five million holes. Through careful optimization of hole size, this "antihole" sieve has holes centered on the dark underlying Fresnel zones. The diffraction-limited performance of a 1 m focal-length, $f/10$ element is demonstrated with a view toward constructing large lightweight telescopes for space applications. © 2007 Optical Society of America

OCIS codes: 050.1970, 350.1260, 110.6770, 090.2890.

1. Introduction

Next-generation space-based telescopes for astronomy, surveillance, and free space optical communications with apertures >20 m will require the development of novel technological approaches. One possibility is to use gossamer membrane optics that can be deployed from very small packages. Most efforts have concentrated on inflatable mirrors, but creating the three-dimensional structures in a weightless environment is difficult, and the concepts are orders of magnitudes away from diffraction-limited surface quality. We are investigating the possibility of using simple diffractive elements using flat membranes. The advantage of this approach is that a well-defined flat can be achieved relatively easily. The diffractive element considered in this case is a photon sieve [1–6] that is based on a traditional Fresnel zone plate (FZP) [7–10]. The photon sieve is superior to the FZP in that no support struts or backing structure is required, so high-contrast imaging can be achieved with no scatter or diffraction spikes. Furthermore, with an even distribution of holes, the substrate can be pulled flat without buckling or wrinkling. The trade-off over a mirror is reduced optical efficiency and severe bandwidth limitations due to dispersion. In this paper we present the design for a broadband photon sieve telescope aimed at addressing both of these issues.

A photon sieve is essentially a FZP in which the rings have been broken up into isolated circular holes. For an infinite conjugate, binary FZP of focal length f at a wavelength λ, the radial distance to the center of the nth bright zone is given by r_n:

$$r_n^2 = 2nf\lambda + n^2\lambda^2. \tag{1}$$

The width w of each zone is such that the area is a constant $\pi\lambda f$, so

$$w = \frac{\lambda f}{2r_n}. \tag{2}$$

In its simplest version, the photon sieve consists of holes of diameter w located at the corresponding radial distance r_n. The holes can be distributed regularly or randomly in angle about the zone. Kipp and others [1–3] have shown that the diameter of the holes can be increased beyond the underlying zone width to permit the construction of a large optic with smaller focal lengths. The effective contribution from a hole size d is given by the oscillating function [5]:

$$F \propto \frac{d}{w} J_1\left(\frac{\pi d}{2w}\right), \tag{3}$$

where J_1 is the first-order Bessel function of the first kind.

A conventional photon sieve will have holes centered on the bright zones. In that case, when $F > 0$,

0003-6935/07/183706-03$15.00/0

light passing through the holes is giving a positive contribution to the focus, and when $F < 0$, the transmitted light is acting to reduce the focused intensity. More simply, we can understand this as in terms of the area of the holes compared to the underlying bright zone [1–5]. Increasing the hole size relative to the underlying bright zone (by a factor d/w) will continue to give a positive contribution toward the focus so long as the overlap with the underlying bright zone is greater than the overlap with any region of the dark zone. In this work, however, we have increased the size of the hole to the negative region of this function, but we have achieved a positive contribution from the hole by positioning the hole on a dark zone. Such an "antihole" configuration permits a hole size as large as 3.514 times the underlying zone width. This in turn leads to the construction of a significantly larger primary without the requirement of impractically small holes or any reductions in throughput from such apertures.

2. Antihole Photon Sieve

An antihole photon sieve was designed with a focal length of 1.0 m and a diameter of 0.1 m to operate at a wavelength of 532.1 nm. The angular positions of 4,999,922 holes were positioned randomly on every second dark zone ($n = 7.5$–2363.5) such that they did not overlap. The holes ranged in size from 19 to 331 μm in diameter, with the largest in the center. Figure 1 shows an image of the central 20 mm diameter of the photon sieve, with rings of order $n = 7.5$–99.5. An electron-beam lithographic process was used to produce the photon sieve on a chrome-coated, 125 mm square, 2.4 mm thick quartz plate. A frequency-doubled, Nd:YAG laser ($\lambda = 532.1$ nm) was spatially filtered and directed onto a high-quality apochromat lens ($f = 715$ mm, $D = 150$ mm) to create a diffraction-limited collimated beam. The performance of the photon sieve was then evaluated in several ways: focusing, imaging, and interferometry.

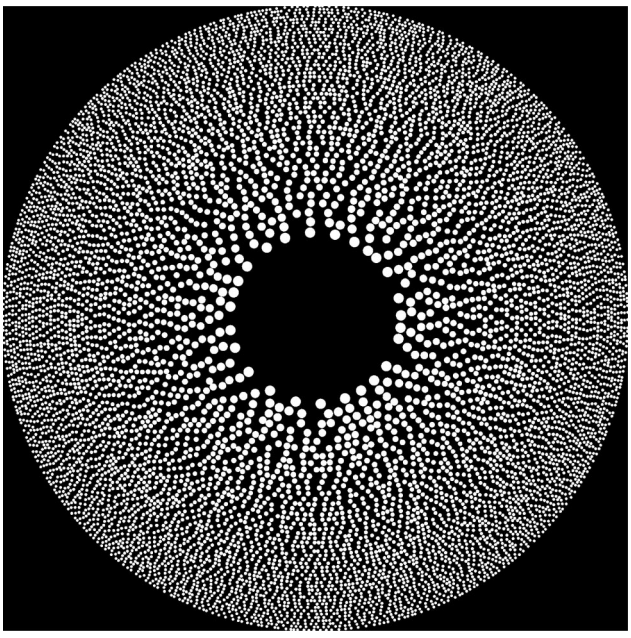

Fig. 1. Central 20 mm diameter of the antihole photon sieve.

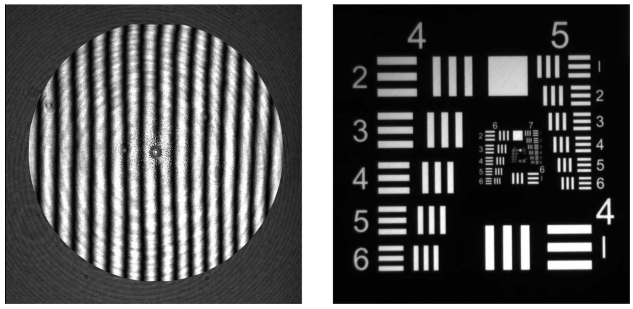

(a) (b)

Fig. 2. (a) Interferogram of the photon sieve. (b) Image of a resolution test target produced by the photon sieve.

The photon sieve produced a focal spot with a total efficiency of 0.2%. The diameter of the central maximum was 12.8 μm compared to the expected diffraction-limited spot size of 13 μm. This slight improvement is most likely because the photon sieve is not a completely filled aperture (in radial terms) but has regular rings absent. The result of this apodization is to reduce the diameter of the Airy spot somewhat. The focused light from the photon sieve was then recollimated with a high-quality achromat and made to interfere with a diffraction-limited reference beam. Figure 2(a) shows the resultant interferogram of the photon sieve. An analysis of the interferogram gave a wavefront error of 0.02λ peak to valley, 0.12λ rms, and a Strehl ratio of 0.98. The actual performance of the photon sieve is most likely better than this interferometric measurement suggests, as it includes the wavefront errors of numerous test optics (three lenses, two mirrors, and one beam splitter).

The spatial filter used for illuminating the collimator was replaced with a 1951 U.S. Air Force resolution test target illuminated by laser light passed through a rotating diffuser to remove speckle. The image of the target produced by the photon sieve at 532.1 nm is shown in Fig. 2(b). In a magnified image of the central region, the cut-off spatial frequency was found to be group 8, element 1 (256 line pairs/mm). The filled-aperture Rayleigh limit for point sources is 154 line pairs/mm. The higher resolution is explained by the three-bar target not being the same as point-source illumination and the Rayleigh criterion being slightly less than the true cut-off frequency.

3. Broadband Operation

The photon sieve is a diffractive element and, as such, suffers from dispersion. In a focusing element such as this, the focal length will change with wavelength according to

$$\frac{\Delta f}{f} = \frac{\Delta \lambda}{\lambda}. \tag{4}$$

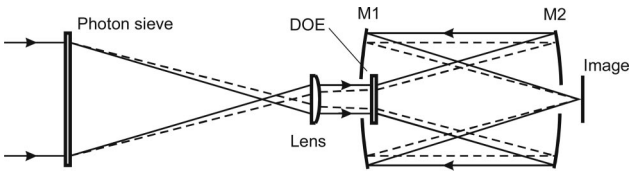

Fig. 3. Optical layout for the broadband photon sieve telescope. The paths of two different wavelengths are shown as solid and dashed.

Using depth of focus considerations, images will remain in focus over a bandwidth given by

$$\Delta\lambda \approx \frac{2\lambda^2 f}{D^2} \tag{5}$$

or a mere 0.06 nm in the case of the photon sieve presented here. In order to obtain a useful bandwidth, a corrective system incorporating a second dispersive element was constructed as shown in Fig. 3. The photon sieve is first reimaged onto a diffractive optic element (DOE) using a lens. The DOE is designed to have the optimal dispersion characteristics to compensate for the dispersion of the photon sieve primary. This results in a divergent beam that needs to be focused to produce an image. This is achieved with two mirrors (M1 and M2).

The broadband configuration was tested experimentally with a hologram constructed in-house as the DOE. A 40 mm diameter phase transmission hologram ($f = -158.5$ mm) was created in bleached silver halide plate film for this purpose. A 400 mm focal-length lens collimated the focused light and imaged the photon sieve onto the hologram. The resultant highly divergent beam was collimated, then refocused using two, 200 mm diameter mirrors ($f =$ 734 mm and 807.7 mm, respectively). Using optical design software, the diffraction-limited ($\lambda/14$ rms) bandwidth for this system was found to be 40 nm ($\lambda = 522$–562 nm).

After construction, the focal spots were tested at laser wavelengths of 514.5, 532.1, and 543.4 nm, respectively, as shown in Fig. 4(a). The focal spots have very little noticeable difference between them. The beams were then tested interferometrically at the first two wavelengths [Figs. 4(a) and 4(b)], while the third laser (a green He–Ne) could not provide sufficient power for this test. Analysis of the interferograms gives Strehl ratios of 0.88 and 0.83 at the wavelengths of 514.5 and 532.1 nm, respectively. Most of this error was due to coma, which should not be present in this setup so long as all the optical components are performing to specifications and are correctly aligned. The wavefront error as measured also incorporates the combined error from six mirrors, three lenses, a beam splitter, and the hologram itself, so it is expected that the true error is better than that given here.

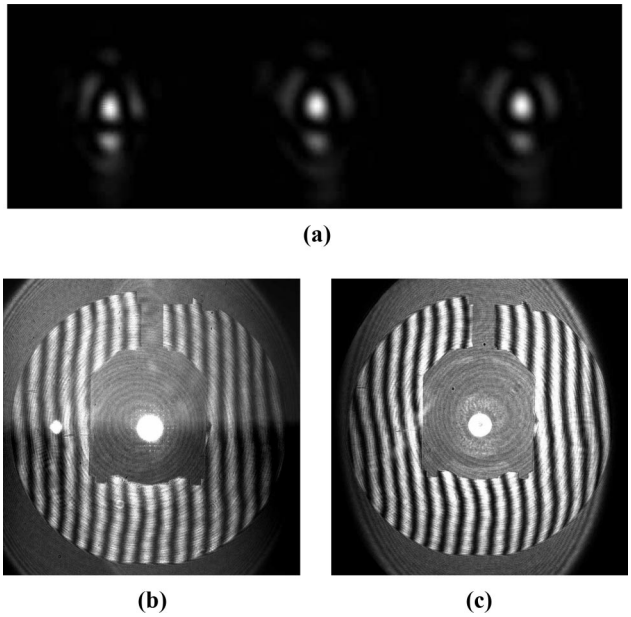

Fig. 4. (a) Focal spots of the broadband antihole photon sieve telescope recorded at 514.5, 532.1, and 543.4 nm, respectively. (b), (c) Interferograms recorded at 514.5 and 532.1 nm, respectively.

4. Conclusion

We have created a telescope consisting of an antihole photon sieve with very large holes centered on "dark" Fresnel zones. This design permits the creation of much larger apertures without sacrificing optical throughput. The telescope was then corrected for dispersion using a secondary diffractive element to operate over a bandwidth of 40 nm. The success of these tests indicates that photon sieves may serve as inexpensive primaries for ultralarge space-based telescopes.

We would like to acknowledge the support of this research by the U.S. Air Force Office of Scientific Research.

References

1. L. Kipp, M. Skibowski, R. L. Johnson, R. Berndt, R. Adelung, S. Harm, and R. Seemann, "Sharper images by focusing soft X-rays with photon sieves," Nature **414,** 184–188 (2001).
2. Q. Cao and J. Jahns, "Focusing analysis of the pinhole photon sieve: individual far-field model," J. Opt. Soc. Am. A **19,** 2387–2393 (2002).
3. Q. Cao and J. Jahns, "Nonparaxial model for the focusing of high-numerical aperture photon sieves," J. Opt. Soc. Am. A **20,** 1005–1012 (2003).
4. Q. Cao and J. Jahns, "Modified Fresnel zone plates that produce sharp Gaussian focal spots," J. Opt. Soc. Am. A **20,** 1576–1581 (2003).
5. Q. Cao and J. Jahns, "Comprehensive focusing analysis of various Fresnel zone plates," J. Opt. Soc. Am. A **21,** 561–571 (2004).
6. G. Andersen, "Large optical photon sieve," Opt. Lett. **30,** 2976–2978 (2005).
7. G. S. Waldman, "Variations on the Fresnel zone plate," J. Opt. Soc. Am. **56,** 215–218 (1966).
8. H. H. M. Chau, "Zone plates produced optically," Appl. Opt. **8,** 1209–1211 (1969).
9. V. E. Levashov and A. V. Vinogradov, "Analytical theory of zone plate efficiency," Phys. Rev. E **49,** 5797–5803 (1994).
10. C. M. Choy and L. M. Cheng, "High-efficiency cosine-approximated binary Gabor zone plate," Appl. Opt. **33,** 794–799 (1994).